
Design and high precision manufacturing of a structural glass scaffolding using glued connection

Paul COVILLAULT*, Niccolo BALDASSINI, Klaas DE RYCKE^{ab}

* Bollinger+Grohmann S.A.R.L., France,
15 rue Eugène Varlin, 75010 Paris, France
pcovillault@bollinger-grohmann.fr

^a Ecole nationale supérieure d'architecture Versailles et LEAV

^b The Bartlett School of Architecture, UCL

Abstract

Réflexion is an art piece designed as a 12m high structural glass scaffolding. It consists of a 1.15m cubic grid of laminated glass bars with a hexagonal section to diffract light. These bars are structurally glued and connected via stainless steel connectors.

The essence of this art piece lies in the juxtaposition of the raw, robust, adaptable, and practical nature of the scaffolding with the purity, precision, and fragility of glass. The marriage of these two antinomic design approaches took place through many project solutions and processes.

The details and assembly process are designed to reduce all eccentricities and imperfections due to fabrication, manufacturing, or erection on-site. Any deviation could cause different load paths and higher local stress concentrations, which the steel could sustain but not the glass or the epoxy glue. For it to function, the design of the node had to be carefully thought through to ensure that every component and material fulfills its predicted role. Besides the high demands on fabrication, the high repetitiveness of the structure provokes a high degree of static indeterminacy, leading to thousands of possible deviations that all need assessment.

The scaffolding idea of easily mountable pieces led us, after multiple explorations, to the design of the on-site bolted stainless-steel node. This connector needs to address manifold challenges, whether it concerns precision in the making, minimal tolerance on site, or resisting high loads. For that, a wax-molded stainless-steel piece, epoxy glued to the glass bar end, is bolted to a welded stainless steel star node. The glass design approach led to the use of high precision technologies and gluing technology derived from the aerospace domain, rarely used in the construction field.

This paper focuses on the design approach, the correlation between design and calculation methods, the correlation between physical and digital prototyping, and the influence of manufacturing knowledge on design and structural design.

Keywords: Structural glass design, structural glazing, Glued glass, Stainless steel molding, high precision manufacturing, Glass connection, Glass testing, Predictability, Artwork

1. Introduction

This research on glass structures and high-strength epoxy glass joints started as a structural engineering study for an artwork: *Réflexion* - a 12 m-high structural glass scaffolding, designed with a French master glassmaker, for a temporary installation in the Tuileries Gardens in Paris, France, for two months, then in Osaka, Japan.

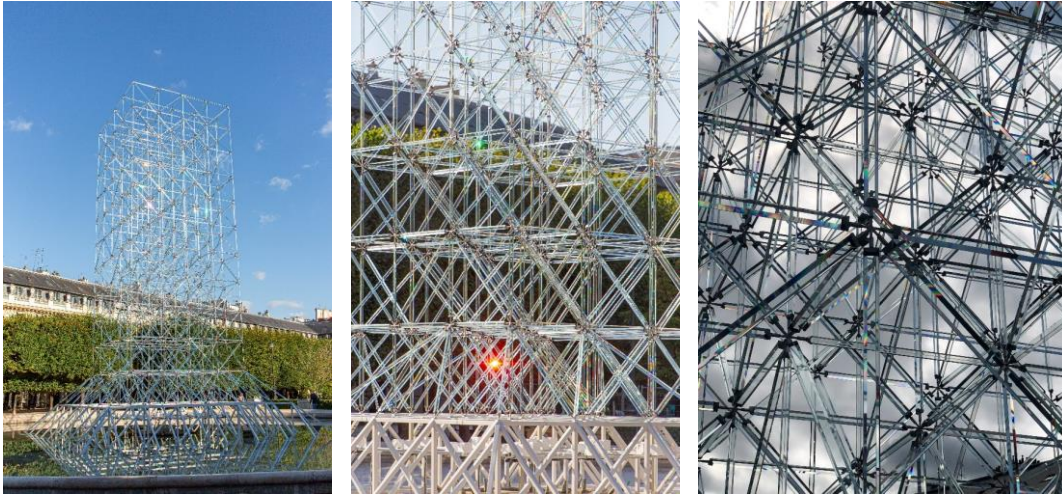


Figure 1: Photos of the completed artwork in the Tuileries Gardens

The art installation consists of a very regular cubic grid, with a 1.15 m mesh. Every bar of this grid is made of two trapezoidal glass plates laminated with a PVB interlayer forming a hexagonal plan that diffracts the light. The grid modules form a 12.65 m high tower on a regular 4.6 m square plan.

The essence of this artwork lies in the opposition between the raw, redundant, and practical nature of scaffolding with the purity, precision, and fragility of glass. The marriage of these two antinomial design approaches gave its body to the final version of the artwork, the design considerations for the connections, as well as to numerous other challenges and design decisions.

Contrary to the perceived simplicity of the scaffolding and its connection system is the structural hyperstaticity or indeterminacy of the system. Its structural system accounts for extreme redundancy, hence multiple possible load paths, which challenges the structural predictability principle of isostatic structures usually used in glass design. In such a brittle structure, the design loads considered for all the calculations must not be exceeded during any stage of the project.

This questions the relationship between the design models of a structure and its actual behavior. Certain differences between modeling and reality are acceptable, and these discrepancies are usually standardized (NF-EN 1090) and accounted for in the design checks (imperfections in the safety coefficients, buckling curves, etc.) or modeled (e.g., for global buckling). In glass structure design, deviations are much more sensitive than for other materials: with such a material having no ductility, any local stress peak due to unexpected load paths can lead to glass failures. This necessitates better predictability of the structure's behavior, hence a finer correlation between the structure and its models.

If the difference between the structure and its model is deemed too significant, models are typically adjusted to align them more closely with reality or to create a broader envelope case that encompasses the actual behavior of the structure. In this work, however, the opposite approach was chosen: to minimize potential deviations within the structure and its components in order to align its behavior more closely with the ideal model.

The underlying article will describe the modeling approaches of the structure at multiple scales: global structure, bar element, and node detail, including their hypotheses, approximations, and limitations. It will also outline the methods used to reduce potential deviations and uncertainty: high-precision manufacturing, specific node design with its assembly process, and laboratory testing.

2. Theoretical models

The design approach for modeling the structure follows a typical process. It involves studying the structure at three distinct scales through separate calculations: the global model, element-scale calculations, and detail studies.

2.1. Global model

The overall structure was designed using Dlubal Rstab, encompassing both the glass superstructure and the steel base. The design followed standard assumptions for perfect trusses: bars are perfectly straight with perfect pins at their ends, axis of multiple crossing members converging in one point, the connection components represented as points rather than fully detailed models. Each element was modeled with its actual section and material properties. This model served to analyze the distribution of forces within the structure and calculate the design loads on all bars, connections, and supports.

Given the specific geometry and materials used, the two most significant approximations in this model are geometric deviations and hyperstatic loads.

Geometric deviations such as the overall inclination of the structure, curvature of straight elements, or axis misalignment can induce parasitic loads in the structure in tension, compression, and bending. While these deviations typically have minimal impact on the load path, they are accounted for in local models used for design checks.

Hyperstaticity effects present a more intricate challenge. In conventional steel, concrete, or wood design, structures can rely on identified possible equilibriums and the material's ductility to ensure safety, even if the load path varies. However, glass structures lack ductility, usually necessitating isostatic schemes to eliminate load path uncertainties and control forces in each member. The artwork studied here, due to its highly hyperstatic nature, complicates this approach. The multitude of deviations, settlement during assembly, and inadvertent tensioning of members make it impractical to account for all potential combinations in the global model while still deriving practical results. Nonetheless, the assembly and fabrication processes were designed to validate the feasibility of this hypothesis.

The finite element (FE) model was then employed to determine the maximum forces acting on bars and nodes: the most heavily loaded bars (vertical bars at the bottom corners, 1.15m long) were found to experience 11.2 kN of tension and 14.8 kN of compression under the ultimate limit state (ULS) wind combination.

2.2. Single glass bar model

The analysis of individual members validates the section of glass bars against tension loads and, critically, buckling, considering the influence of load duration and the PVB joint.

Following geometric explorations of various cross-sections of the bar, which are not detailed here, the design was finalized with a hexagonal shape measuring 60 mm by 39.2 mm.

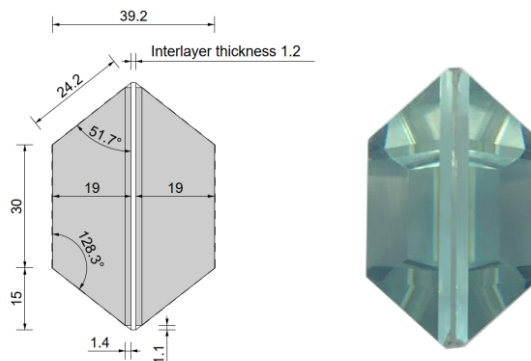


Figure 2: Cross-section and front view of the glass bar

The evaluation of the resistance of such elements is well documented in norms, [1], and gives a tension capacity of the bar of 34.7 kN for wind load combinations.

The buckling capacity of the laminated glass bar is calculated using [2], assuming short-term loading as wind is the leading combination. The formulas of the §6.4.2.2. account for the equivalent inertia of the laminated plates according to the Wölfel-Bennison model for deflection effective thickness, in the Euler critical load of the element. The compression design values are detailed in the table below.

length (end to end of glass)	Buckling capacity	Compression load
0.95 m	20.7 kN	14.8 kN
1.43 m	14.8 kN	14.2 kN
1.79 m	11.8 kN	10.3 kN

Table 1: Buckling capacity and loads of the different bars

As stated by the guide, the buckling phenomenon is highly influenced by tolerances, deviations, and the actual behavior of materials. However, the applicability of the calculation regarding these influences is not clearly outlined. To eliminate any doubts about the buckling capacity of the bars, laboratory tests were conducted to confirm the calculated values.

2.3. Node model

For the connection design, the erection process of the scaffolding, reusability of the structure, and load concentration at the intersection of the bars quickly called for a central stainless-steel node to which the bars would be attached, inspired by Konrad Wachsmann’s universal node technology. The nodes were designed as stainless-steel stars with threaded ends to allow the bars to be screwed onto them.

Regarding the connection of the glass bars to the nodes, a connector is attached to each end of the bar, which allows on-site screwing: a wax-molded stainless-steel piece with a threaded end.

To design this connector, investigations into mechanical joints and silicon adhesive quickly showed to be inadequate. The stress concentrations around mechanical pins or the minimal area necessary to limit the stress in the silicone to an acceptable value imply significant increases in the cross-section. Therefore, the design incorporates a high-strength epoxy joint. The adhesion between the two parts is achieved using Araldite 4858 epoxy (tensile strength of 31 MPa and Young's modulus of 1.6 GPa).

The design principle of the connection is to maximize the adhesion area and utilize the epoxy primarily for shear stress, which is the most favorable behavior of epoxy. The inclination of the adhesive planes towards the bar provides a larger adhesion area, thereby reducing stress in the epoxy joint – both axial and shear. A more inclined plane would have concentrated the stress in shear only, but this was impractical from a glass machining perspective.

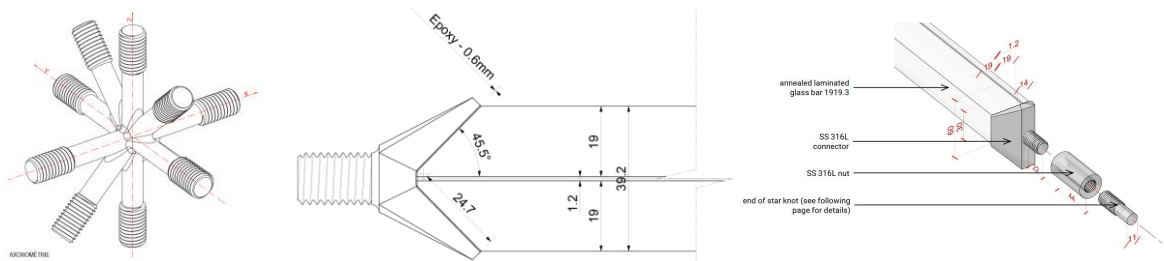


Figure 3: Star node axonometry, Connection geometry between stainless steel and glass bar

Adhesives such as epoxy have been explored in experimental ways [3], but their use remains marginal, despite offering much greater resistance than silicones. The challenge in structural bonding between two different materials with epoxy lies in scientifically assessing the capacity of the entire connection. Two

different approaches were used and compared to converge on the design and analyze the connection's capacity.

The first calculation approach is carried out using [4] and [5] to manually determine the tensile strength of the connection. The stress in the adhesive is calculated assuming a uniform distribution, and is checked by comparing the von Mises stress with the factored capacity.

According to [4], the partial safety factor for materials is $\gamma_m = 1.6$. The simplified design approach for lap joints also incorporates an additional safety factor of 5.0 to account for the non-uniform stress distribution within the connection. This results in a calculated axial capacity of the joint of $N_{t,Rd} = 6.6$ kN. However, this result lacks reliability.

The design guides previously mentioned establish safety factors to address uncertainties in product properties, manufacturing processes, and installation conditions, but they do not explicitly outline their application limitations. Given the unique shape, forces, and materials involved in the node design, there is a significant likelihood that it deviates from the general calculation approaches provided in these guides. Moreover, the safety factor applied to accommodate the uniform stress distribution hypothesis is generic and not related to particular configurations, making it challenging to accurately assess the magnitude of the safety margin. Consequently, this approach was primarily utilized for comparing different configurations and components rather than precisely determining capacity. To achieve a more precise and higher capacity assessment, an alternative approach was employed.

The second approach aims to gain a deeper understanding of the connection's behavior and capacity. It involves using volumetric finite element models to analyze stress peaks and their distribution, as well as to assess the influence of thermal expansion.

This model is built using Dlubal Rfem finite element software. It analyzes the exact theoretical geometry of the connector, encompassing the adhesive thickness and the glass bar geometry. The only simplification involves the PVB joint: since the focus is on the adhesive and its interfaces, the PVB joint is omitted from the model, and the glass bar is considered monolithic. With this model, the stress distribution arising from axial and thermal loads is accurately determined.

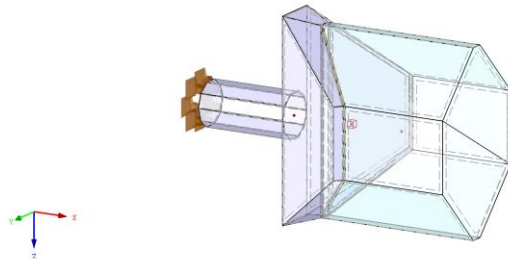


Figure 4: FE volumetric model of connection

The maximum Ultimate Limit State (ULS) axial load (wind) from the global model is considered at 14.8 kN. Thermal loads account for the differential expansion rates of the two materials under sunlight.

Axial load peaks are predominantly situated in the central zone of the connector, following the direct force flow from the glass to the star node. In contrast, thermal load peaks are observed at the outer corners of the connector. The load peaks from these two effects occur at different points within the connection and do not amplify each other.

For comparison, based on [5], without considering the safety factor for uniform stress distribution, the allowable stress in the adhesive would be 19 MPa.

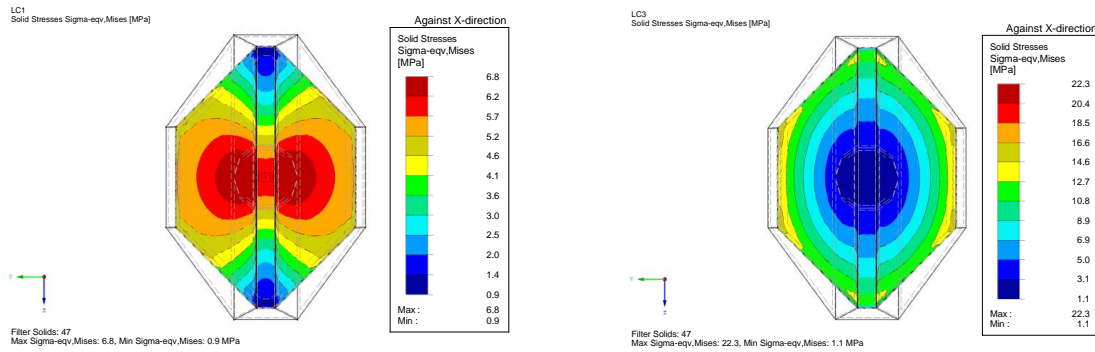


Figure 5: Von Mises stress in the adhesive under axial load and thermal expansion

While this geometrically accurate modeling highlights stress concentration zones and material behavior, it has limitations in definitively assessing the connection's safety. Epoxy's actual behavior is complex and challenging to model [6], especially with finite element software primarily designed for structural engineering. Therefore, a linear elastic behavior assumption was applied to this material, independent of temperature. Geometric imperfections were also not included in the model.

The interpretation of volumetric results in glass design lacks documentation in the literature. Moreover, [5] restricts these analyses to understanding connection behavior and enhancing their capacity. Assessing actual capacity is considered too complex and insufficiently documented for the designer to solely rely on such calculations.

Nevertheless, it remains feasible to anticipate the design's compatibility with the project, as the model indicates a slight margin between the node's capacity and the design load. Therefore, as outlined below, high precision manufacturing reduces uncertainties in deviations and brings the node's actual behavior closer to the anticipated performance. Subsequently, laboratory tests represent the final step to definitively assess the designed node's capacity.

3.Reduction of uncertainty between model and reality

It is widely acknowledged that a certain disparity between modeling and real-world performance is acceptable. Eurocodes outline structural verification processes that accommodate tolerances and precision as per NF-EN 1090. However, as mentioned earlier, existing literature and norms provide insufficient information to safely ensure the design. To address this gap, the chosen method involves adapting the design to achieve closer alignment between actual behavior and theoretical predictions.

The reduction of structure deviation and uncertainty focuses on three parameters: minimizing local deviations, eliminating parasitic loads caused by hyperstaticity, and reducing uncertainty in bars and nodes capacities through laboratory testing.

3.1. Limitation of construction deviations: high precision manufacturing

To minimize all local deviations, high precision manufacturing techniques from the aerospace industry are employed.

Beginning with the most local effect, it is anticipated that the stress distribution in the adhesive and glass edge may deviate from the model due to geometric variations in the bonding surfaces. To ensure a high level of planarity and precision in the angle between the two bonding surfaces, the latter are milled using high-precision machines. Each connector undergoes 3D scanning to verify compliance to specified tolerances ($\pm 0.7\%$ for dimensions larger than 25 mm, following limit deviation js-13 as per IO 286-2 for smaller dimensions, and $\pm 1^\circ$ for surface angles).



Figure 6: Brut wax-casted connector and rectified connector

The construction of the star nodes also adhered to a high-precision process: high-precision negatives were employed to adjust the threaded bars before welding, and each node underwent 3D scanning to verify precision, ensuring tolerances of ± 0.25 mm for all dimensions and $\pm 0.55^\circ$ for all angles.

Regarding the glass, the techniques employed by the glassmaker, including glass polishing, achieve a precision of ± 0.5 mm in the length of the glass. Each bar end undergoes testing with a high-precision negative piece to ensure angles receiving the connectors exhibit no deviation.

These measures effectively reduce uncertainties regarding the nodes' capacity to withstand specified loads. By minimizing deviations in adhesive surfaces, the risk of stress peaks in the glass is reduced, along with moments resulting from local deviations between theoretical axes and actual centerlines. This approach limits potential uneven distribution of stress in the connections.

3.2. Limitation of assembly deviations: Isostatic assembly

On the flip side of uncertainty lies the magnitude of forces transmitted through the nodes. While the structure's redundancy inherently ensures safety, hyperstaticity introduces uncertainty into the force flow critical for glass structures. A crucial factor to address this uncertainty is the assembly process: ensuring no settlement in the pieces, preventing internal stresses from locking during erection due to accidental tensioning or lack of tolerance recovery.

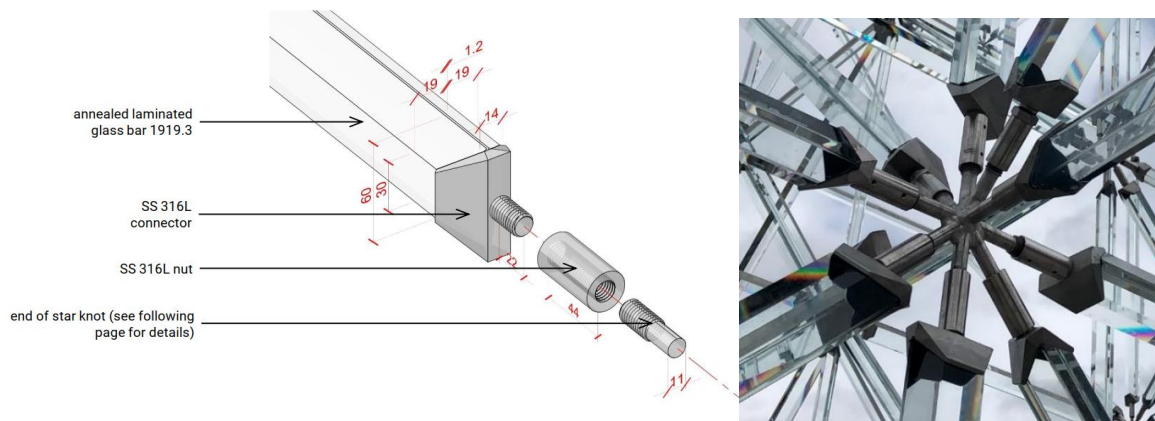


Figure 7: Assembly process axonometry and node photography

The connection between the star node and the glass-mounted connector is achieved using a cylindrical nut. The nut is screwed onto the star node up to its center before the glass bar is introduced. Subsequently, it is rotated to unscrew from the star node and then screwed onto the connector until it makes contact with its flat surface. The length of the cylinder is precisely calibrated to ensure adequate coverage of the star node, accounting for tolerance recovery during the mounting process.

To prevent rotation of the bar around its axis, the entire bar is rotated until one of the connectors engages with the end of the star node inside the nut. Diagonals have a slightly different approach: one of their cylinder nuts and connectors feature inverted threads to accommodate length adjustment. A flat counter-nut is then used to secure and prevent rotation.

This process ensures control over the following parameters:

- Preventing assembly settlement: The cylindrical nut's contact with the connector, the connector's contact with the star node inside the cylindrical nut, and the use of a counter-nut for diagonals ensure that no settlement occurs during assembly. This setup directs any load through the structure along paths of relative rigidity.
- Avoiding parasitic tensioning during erection: Parts are positioned before connections are secured, and the locking process involves only identical movement on both sides of the bar as it rotates. This method ensures no tension or compression is generated by tightening the nut.
- Limiting Parasitic Stress: The cylindrical nuts are hand-tightened, naturally restricting torque and thereby minimizing any parasitic stress.

Another safety measure based on feedback from the full-scale mock-up involves the cylindrical nuts that connect the connectors and the star node: They are manufactured to two standard accuracy classes according to ISO 286-2. The majority are precision class E, allowing for small angle tolerances while ensuring secure connections. Another set of screws with a looser tolerance class (class C) is used in cases where slight resistance during screwing indicates local parallelism deviation.

Implementing these measures has effectively limited the effects of deviations, assembly settlement, or accidental tensioning during member mounting. This validation ensures that the theoretical global model, despite neglecting these effects, closely aligns with the actual behavior of the structure, thereby reducing uncertainty regarding maximum loads on any member or connection.

3.3 Laboratory tests

The final method employed to reduce uncertainty between calculations and reality involved conducting laboratory tests. The tests encompassed all imperfections and deviations within the nodes, thereby exposing any critical failure modes that might arise.

The initial series of tests focused on validating the axial capacity of the glass bars and their connectors. Small samples of bars were manufactured, and connectors were glued on both ends following the selected process for the artwork.

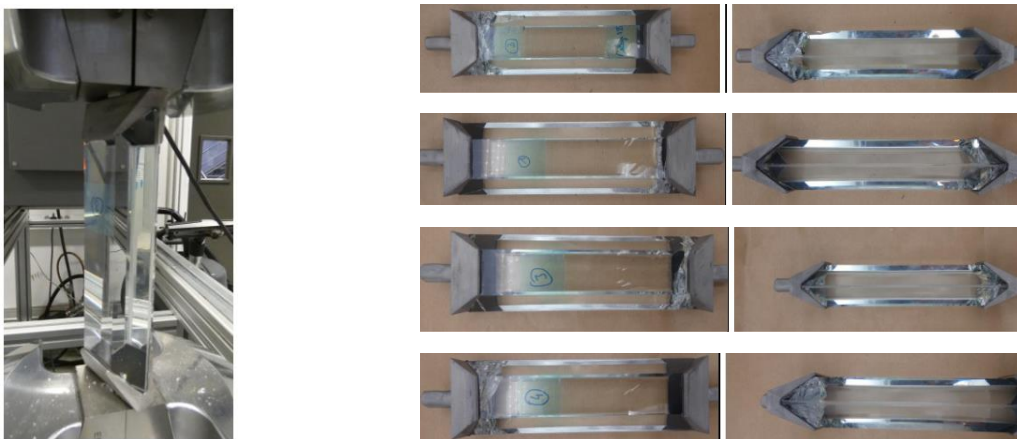


Figure 8: Left: tensile test configuration / Right: Photographs of fracture patterns.

The results indicated an average failure load of 35.6 kN, with a standard deviation of 3.6 kN (minimum 30.5 kN, maximum 39.5 kN).

The second test focused on determining the buckling capacity of the bars. Laboratory tests were conducted on the longest type of bar in the structure, specifically the 1.43 m bars of the diagonals in the grid. The test involved applying an increased load of 3 kN/min while measuring the axial deformation at the top of the bar.

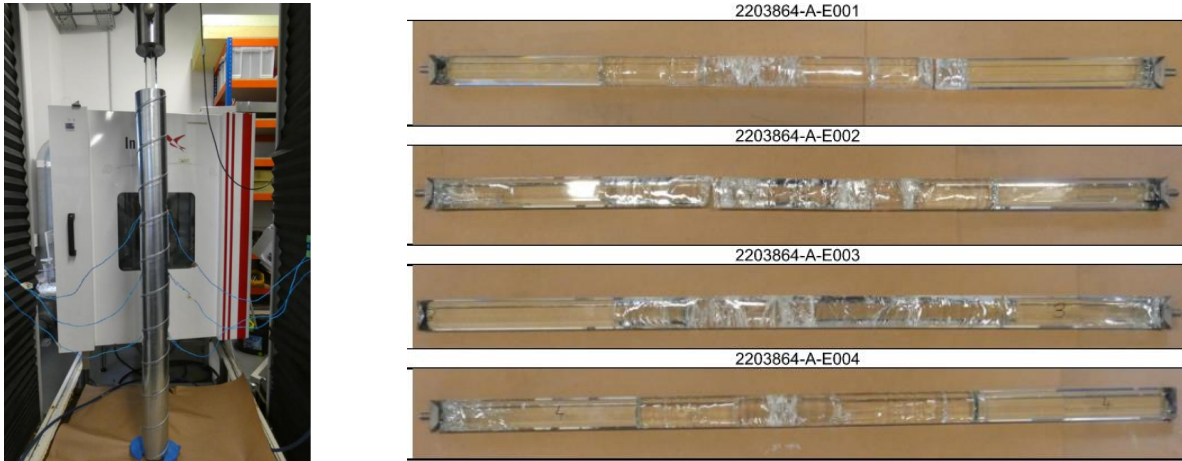


Figure 3: Left: Buckling test configuration / Right: Photographs of fracture patterns.

The test results consistently showed a similar mode of failure (flexural buckling, breakages at the center of the bar) and uniform capacity: the mean failure load was 77.7 kN with a standard deviation of 6.6 kN (minimum 70.7 kN, maximum 88.6 kN).

The allowable forces are then calculated using §D.7.3 of NF EN 1990-1. This calculation employs a simple statistical approach that requires the designer to select a conversion coefficient to account for uncertainties not covered by tests. Since the tests were conducted on real bars and connectors, this coefficient can be taken as 1.0. Therefore, the tension capacity of the bars and their connectors is $N_{Rd} = 19.5$ kN, providing an additional safety margin of 30% relative to the maximum load predicted by the global model.

Regarding the buckling capacity of diagonal members, it was determined to be $N_{Rd} = 49.7$ kN. This value significantly exceeds the one predicted by standard calculations. There are two main reasons for this disparity: first, the test defines failure as the point of instability, whereas fractures could already be observed in the glass at lower loads. Secondly, standard calculations consider short-term loading (such as wind), whereas buckling is an instantaneous phenomenon that occurs with a stiffer behavior of the PVB layer, resulting in a higher equivalent inertia of the section.

The tests affirmed the results of the studies conducted to assess the capacity of the connections and the minimum capacity of all elements in the structure.

4. Discussion

The erection on site began on August 16th and lasted for 4 weeks. The artwork was displayed in the Jardin des Tuileries in Paris from September 15th, 2023 to November 15th, 2023, after which it was dismantled. Throughout this period, the outside temperatures fluctuated between 5°C and 35°C, and Paris experienced storm Cynthia with local winds reaching up to 17.5 m/s (averaged over 10 minutes). Despite these conditions, the structure remained intact without any damage.

This demonstrates that the engineering approach, where the design of the nodes and construction process was tailored to fit the theoretical model rather than vice versa, proved to be effective for glass design.

It also serves as a proof of concept for the simplicity of assembly. The entire structure, including the steel base, was erected by a contractor specialized in special steel structures (though not in glass) in just 4 weeks, and later dismantled within a fortnight, demonstrating both its ease of assembly and durability.

The application of epoxy at the glassmaker's facility, rather than in a controlled laboratory environment, underscores the newfound potential of high-strength epoxy adhesives for glass connection designs in architecture. This extends beyond research projects, offering promise for broader application in practical settings.

However, a local failure is still to be noted: observed in a small number of bars, where cracks near the connectors appeared. The exact cause of these cracks remains undetermined.

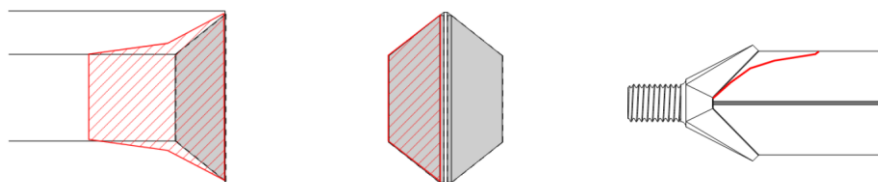


Figure 13: Crack geometry in the glass

This failure did not compromise the structure's safety, thanks to its redundancy and the safety design incorporating laminated glass. The structural redundancy ensures robustness and enables it to withstand such incidents. As is often the case with hyperstatic structures, challenges arise during conception but are mitigated by the structure's inherent safety.

This sculpture underscores the delicate balance that designers must strike in glass structures: ensuring security through redundancy while grappling with the predictability challenges posed by hyperstaticity.

5. Conclusion

This work demonstrates the successful realization of a pioneering glass structure with a high-strength epoxy bond between glass and stainless steel. The achievement of sufficient bonding strength and resistance comparable to glass properties opens new perspectives for epoxy-bonded glass structures.

Furthermore, it showcases an alternative approach to overly complex modeling through intelligent design and high-precision manufacturing techniques.

Additionally, it underscores the limitations of existing glass design approaches when applied to specific glass structures and raises questions about the applicability of generic norms and standards in glass design.

References

- [1] PR NF EN 16612- Glass in building — Determination of the load resistance of glass panes by calculation and testing
- [2] CNR – Advisory Committee on Technical Recommendations for Construction -DT 210/2013 Guide for the Design, Construction and Control of Buildings with Structural Glass Elements, Roma -CNR (2013)
- [3] Blandini Lucio - Structural Use of Adhesives in Glass Shells. VERLAG GRAUER, Beuren und Stuttgart, 2005.
- [4] The institution of Structural Engineers, Guide to the structural use of adhesives. SETO, London (1999)
- [5] The European structural polymeric composites group - Structural Design of Polymer Composites. John Clarke, London (1996)
- [6] Dean G., Crocker L. - The Use of Finite Element Methods for Design with Adhesives. National Physical Laboratory, Teddington (2001)
- [7] Müller M., Herák D., 2010. Dimensioning of the bonded lap joint. Res. Agr. Eng., 56: 59–68 (2010)